Bursting as an emergent phenomenon in coupled chaotic maps

Gerda de Vries*
Department of Mathematical and Statistical Sciences, University of Alberta, Edmonton, Alberta, Canada T6G 2G1
(Received 26 June 2001; published 25 October 2001)

A two-dimensional map exhibiting chaotic bursting behavior similar to the bursting electrical activity observed in biological neurons and endocrine cells is examined. Model parameters are changed so that the bursting behavior is destroyed. We show that bursting can be recovered in a population of such nonbursting cells when they are coupled via the mean field. The phenomenon is explained with a geometric bifurcation analysis. The analysis reveals that emergent bursting in the network is due to coupling alone and is very robust to changes in the coupling strength, and that heterogeneity in the model parameters does not play a role.

DOI: 10.1103/PhysRevE.64.051914 PACS number(s): 87.19.Nn, 05.45.Xt

I. INTRODUCTION

In the context of this paper, an emergent phenomenon is a phenomenon observed in a population of cells that cannot be predicted readily from the properties of its individual constituents. Emergent phenomena, such as the generation of oscillations from nonoscillatory cells via gap-junctional coupling [1–4], have been of interest for some time in neurobiological and endocrine systems. Neurons and endocrine cells rarely act alone, but rather as members of a population connected together via gap-junctional or synaptic coupling. Thus, the electrical activity observed in the population is the result of the properties of individual cells as well as of the nature of the coupling.

In this paper, we are interested in emergent bursting from nonbursting cells. Bursting is a complex oscillation of the membrane potential of cells, characterized by a periodic alternation between active and silent phases. During the silent phase, the membrane potential is at a quasisteady state, whereas during the active phase it undergoes rapid oscillations. Bursting oscillations are commonly seen to be the primary mode of behavior in a wide variety of neurons and endocrine cells, such as pancreatic β cells [5], hippocampal pyramidal neurons [6], and thalamic neurons [7].

Most models describing bursting in single cells consist of a system of nonlinear ordinary differential equations, and the dynamics of these systems are well understood. Following the analysis of Rinzel [8,9], bursting activity is typically viewed as being the result of the interaction of a fast and a slow subsystem. The fast subsystem can exhibit rapid oscillations (active phase) and stable steady states (silent phase). The slow subsystem is responsible for switching the dynamics of the fast subsystem between these two states in a periodic fashion.

There are now several theoretical papers in which bursting as an emergent phenomenon, resulting from gap-junctional coupling of nonbursting cells, has been demonstrated. The nonbursting cells are related to the bursting cells in the sense that the parameter regimes in which each type exists are relatively close. Thus, changes in a few key parameters can turn a bursting cell into a nonbursting cell, and vice versa. Implications of the phenomenon have been discussed in the context of electrical activity of pancreatic β cells; however, they are equally applicable to comparable systems. Two types of emergent bursting must be distinguished. First, Smolen *et al.* [10] proposed the heterogeneity hypothesis, in which cell parameters are randomly distributed so that only a few cells can burst. When coupled diffusively, the population as a whole takes on the properties of the average cell, provided the coupling strength is sufficiently strong. As long as the average cell bursts, the population bursts. A similar concept was put forward by Cartwright [4] and by Manor *et al.* [3] in their studies of emergent oscillations from silent cells by gap-junctional coupling. Second, Sherman and Rinzel [2] and Sherman [11] demonstrated that identical nonbursting cells (so the average cell is a nonbursting cell as well) can be converted to bursting cells by weak gap-junctional coupling. The emergent phenomenon exists only for a small range of coupling strengths, but can be enhanced either by the addition of noise [12] or by the addition of heterogeneity in the cell parameters [13].

In this paper, the investigation of the second type of emergent bursting is continued with the examination of a two-dimensional map, recently introduced by Rulkov [14], that produces chaotic bursting patterns similar to those observed in neurons and endocrine cells. The map is a caricature of the Hindmarsh-Rose model of a biological neuron [15]. Rulkov used the map to demonstrate and explain the onset of regular bursts in a group of irregularly bursting neurons with different individual properties when they are coupled to each other through the mean field. Here, we extend Rulkov's analysis with a careful bifurcation study, and show that the coupled map can also support emergent bursting from nonbursting cells. In contrast to the findings with previously studied continuous systems, coupling alone is sufficient, the phenomenon is robust for a large range of coupling strengths, and heterogeneity does not play a key role.

In Sec. II, the map representing a single cell is introduced, and the dynamics of the single cell are explained via a one-dimensional geometric bifurcation analysis. To understand the mechanism responsible for emergent bursting from nonbursting cells, it helps to first examine the effect of mean field coupling on a pair of bursting cells, which we do in Sec. III. Then, in Sec. IV, emergent bursting is demonstrated and

*Email address: devries@math.ualberta.ca
URL: http://www.math.ualberta.ca/~devries

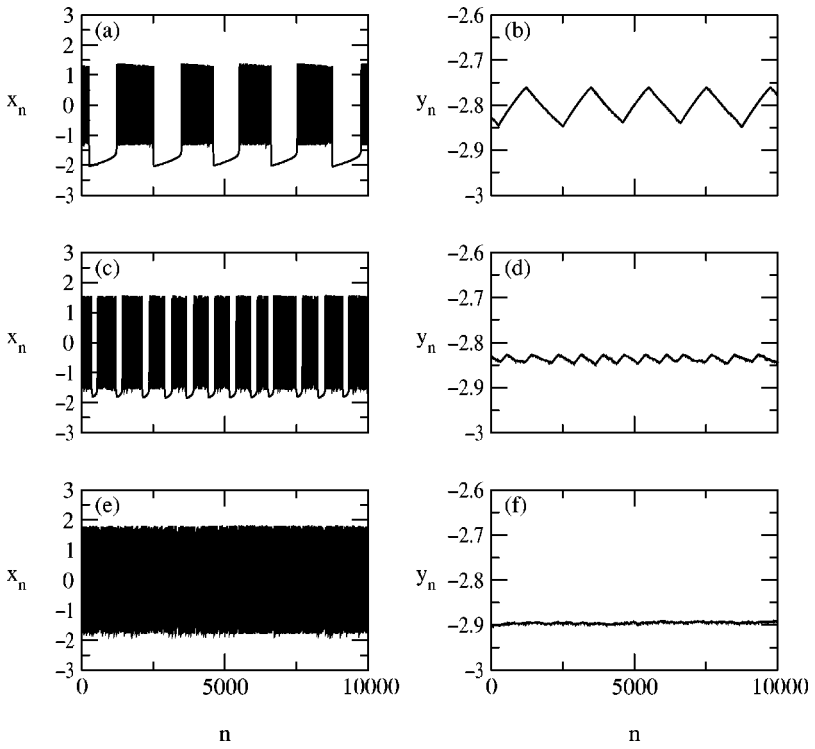

FIG. 1. Behavior of the single-cell model (1), (2). (a) and (b) $\alpha=4.15$; (c) and (d) $\alpha=4.4$; (e) and (f) $\alpha=4.7$. Other parameter values are $\eta=0.0001$ and $\sigma=-1$.

explained, and the role of heterogeneity in model parameters is examined in Sec. V. Finally, we compare the mechanisms underlying emergent bursting in previously studied continuous systems and this map in Sec. VI.

II. THE SINGLE-CELL MODEL

The behavior of a single cell is described by the following two-dimensional map [14]:

$$x_{n+1}=\frac{\alpha}{1+x_n^2}+y_n, \tag{1}$$

$$y_{n+1}=y_n-\eta(x_n-\sigma), \tag{2}$$

where α, η, and σ are parameters. Both α and σ are $\mathcal{O}(1)$, and $0<\eta\ll 1$. A few typical wave forms for Eqs. (1), (2) are shown in Fig. 1. Following the terminology used for bursting solutions obtained from continuous systems [9], we will refer to the wave forms shown in Figs 1(a) and 1(c) as square-wave bursting, and to the wave form shown in Fig. 1(e) as spiking. Other wave forms, such as tapered bursting [16,17], are possible for other values of α, but we will not discuss those here.

The solution behavior of Eqs. (1), (2) can be explained by means of a geometric bifurcation analysis. Since $0<\eta\ll 1$, the time course of y_n is much slower than that of x_n. Thus, we can study the dynamics of the fast subsystem (1) by treating y_n as a parameter, viz.,

$$x_{n+1}=R(x_n)=\frac{\alpha}{1+x_n^2}+\gamma. \tag{3}$$

This approach was pioneered by Rinzel [8] in a study of continuous bursting systems, and was also employed by Rulkov [14] in his analysis of Eqs. (1), (2), although the dynamics of Eq. (3) are not summarized in a bifurcation diagram in [14].

For each value of the parameter γ, one can determine the fixed points of the map (3) and their stability. The curve of fixed points, given by $R(x_n)=x_n$, traces out an S shape in the (γ,x_n) plane, as shown in Fig. 2(a). Saddle-node bifurcations (denoted by open circles) occur at the knees of this curve. The right saddle node is of particular importance, and we will refer to the value of γ at which this bifurcation occurs as γ_{SN}. Fixed points on the bottom branch are always stable, and fixed points on the middle branch are always unstable. The stability of the fixed points on the upper branch changes at period-doubling bifurcations (denoted by filled squares). For values of γ near the period-doubling bifurcations, stable two-cycles are observed. The two-cycles become four-cycles, eight-cycles, etc., in a fashion similar to the well-known logistic map [18], and eventually the periodic attractors give way to chaotic attractors. Periodic windows can be observed for small intervals of the bifurcation parameter γ. The thick solid C-shaped and backward C-shaped curves indicate the theoretical maximum and minimum iterates (not necessarily realized), given by

$$x_n=R(0)=\alpha+\gamma, \tag{4}$$

$$x_n=R(R(0))=\frac{\alpha}{1+(\alpha+\gamma)^2}+\gamma, \tag{5}$$

respectively. External crisis bifurcations (denoted by filled circles) occur when the minimum iterate maps onto an un-

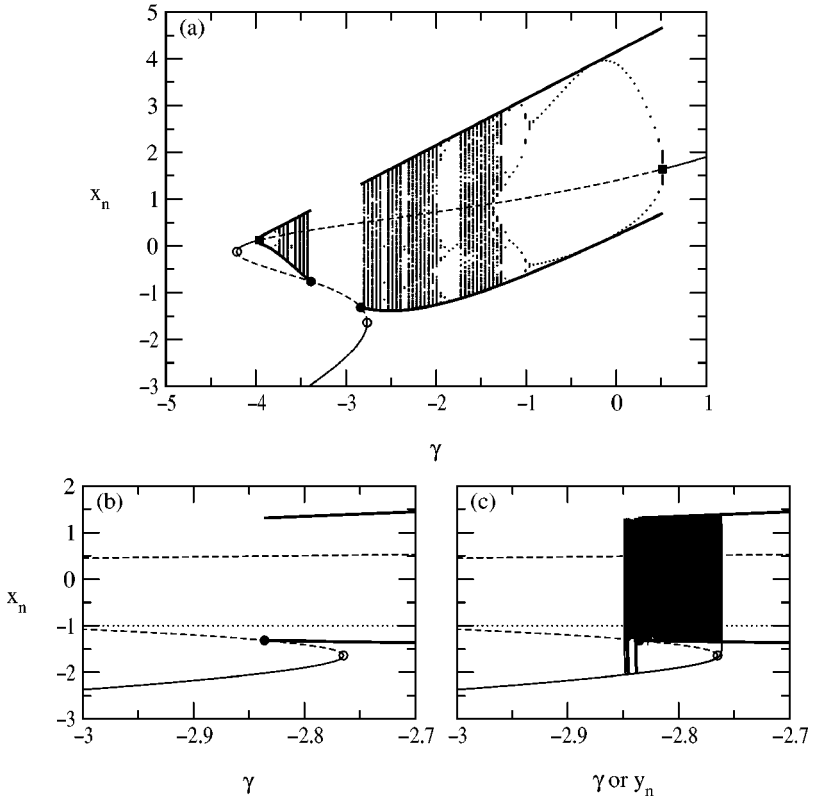

FIG. 2. (a) Bifurcation diagram for the single-cell fast subsystem (3), using γ as the bifurcation parameter, with $\alpha=4.15$. The S-shaped curve is the curve of fixed points (thin solid lines indicate stable fixed points and dashed lines indicate unstable fixed points). Dots denote periodic and chaotic iterates of the one-dimensional map (for 100 values of γ between the left and right period-doubling bifurcations; for each value of γ, approximately 300 iterates are shown). Thick solid lines represent $x_n=R(0)$ and $x_n=R(R(0))$, the theoretical maximum and minimum iterates, respectively. Open circles denote saddle-node bifurcations; filled squares denote period-doubling bifurcations; filled circles denote external crisis bifurcations. (b) As (a), but without the periodic and chaotic iterates, for the values of γ of interest for a bursting solution. The y_n nullcline $x_n=\sigma$ is superimposed and shown as a dotted line. (c) As (b), with the wave form of the full single-cell model superimposed.

stable fixed point on the middle branch of the curve of fixed points, that is, when the curve represented by $x_n=R(R(0))$ intersects the middle branch. Of particular importance is the external crisis bifurcation on the right, and we will refer to the value of γ at which this bifurcation occurs as γ_{EC}.

The key to bursting is the fact that there is a range of values of the bifurcation parameter γ for which there is bistability. In particular, for $\gamma_{EC}<\gamma<\gamma_{SN}$, there is bistability between stable fixed points on the bottom branch of the S curve, corresponding to the silent phase of bursting, and periodic and/or chaotic attractors between the curves $x_n=R(0)$ and $x_n=R(R(0))$, corresponding to the active phase of bursting. This region is shown in more detail in Fig. 2(b). If we now include the dynamics of y_n, the mechanism underlying bursting becomes clear. Note from Eq. (2) that y_n does not change when $x_n=\sigma$ [dotted line in Fig. 2(b)], and that y_n increases (decreases) when $x_n<\sigma$ ($x_n>\sigma$). In Fig. 2(c), the wave form shown in Figs. 1(a) and 1(b), obtained from the full single-cell model, is projected onto the bifurcation diagram of the fast subsystem. During the silent phase, iterates of the map are at or near the stable fixed points on the bottom branch of the S curve, and below the line $x_n=\sigma$. Thus, y_n is slowly increasing. The switch to the active phase is made when y_n moves to the right of the right saddle-node bifurcation, that is, when $y_n>\gamma_{SN}$. During the active phase, iterates lie above the line $x_n=\sigma$ on average, and so y_n is slowly decreasing here. The switch back to the silent phase is made when $y_n\approx\gamma_{EC}$. The accuracy with which the dynamics of the full two-dimensional map can be predicted by the bifurcation diagram for the one-dimensional fast subsystem depends on the magnitude of the parameter η in Eq. (2). The smaller η, the slower the dynamics of y_n, and the better the prediction. Due to the fact that the attractor surrounding the unstable fixed point is chaotic near $\gamma=\gamma_{EC}$, the actual transition from the active to the silent phase can be delayed. Small delays in the return to the silent phase are visible in Fig. 2(c).

Varying the value of α affects the bifurcation diagram for Eq. (3). Of particular importance are the positions of the bifurcation points relative to each other. This information is summarized in the two-parameter bifurcation diagram shown in Fig. 3. By traversing the thin dotted horizontal line at $\alpha=4.15$ from left to right, the six bifurcation points shown in Fig. 2(a) are encountered in order. It can be seen that decreasing α from 4.15 causes the distance between γ_{EC} and γ_{SN} to be increased. That is, the region of bistability is enlarged, resulting in longer active and silent phases. Then, a delay in the switch from the active to the silent phase affects the duration of the silent and active phases only in a minor way, and so the bursting is nearly periodic. When $\alpha=4$, the external crisis points coalesce and disappear. At this point, the two branches of $x_n=R(R(0))$ join, and square-wave bursting gives way to tapered bursting [16,19]. On the other hand, increasing α from 4.15 causes the region of bistability to be diminished, resulting in shorter active and silent phases [compare Figs. 1(a) and 1(c)]. Then, a delay in the switch from the active phase to the silent phase due to the chaotic nature of the attractor near γ_{EC} is particularly noticeable, and the bursting is no longer nearly periodic. When $\alpha=8\sqrt{3}/3$, γ_{EC} coincides with γ_{SN}. At this point, there is no longer any bistability. Depending on the parameter values of Eq. (2), a bursting wave form can be obtained, but in general the two-dimensional map produces either a wave form with fast

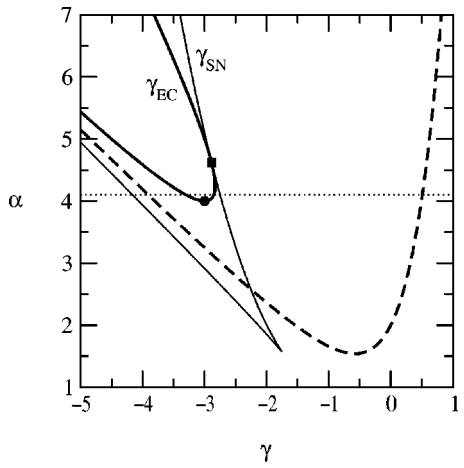

FIG. 3. Two-parameter bifurcation diagram for the single-cell fast subsystem (3). The thin solid line represents the curve of saddle-node bifurcations, given by $\alpha=-2[(\gamma^2+9)\gamma\pm(\gamma^2-3)^{3/2}]/27$ [14]; the thick dashed line represents the curve of period-doubling bifurcations, given parametrically by $\alpha=(x^4+2x^2+1)/(2x)$ and $\gamma=(x^2-1)/(2x)$; the thick solid line represents the curve of external/internal crisis bifurcations, given by $\alpha=-(3\gamma\pm\sqrt{\gamma^2-8})/2$ [14]. The filled square at $\alpha=8\sqrt{3}/3$ indicates the tangential intersection of the right saddle-node and external crisis curves. The bullet at $\alpha=4$ indicates the coalescence and disappearance of the two external crisis points as α is decreased. The thin dotted horizontal line given by $\alpha=4.15$ corresponds to the situation analyzed in Fig. 2.

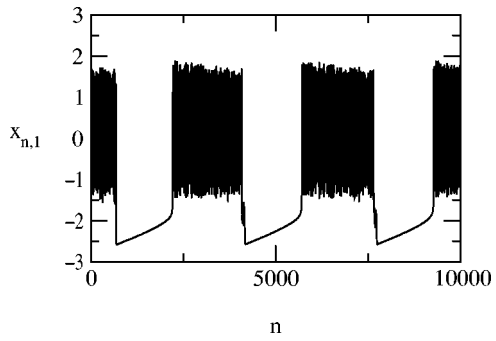

FIG. 4. Wave form of the two-cell model (6), (7), with $\alpha_1=\alpha_2=4.15$ and $\varepsilon=0.2$. Other parameter values are $\eta=0.0001$ and $\sigma_1=\sigma_2=-1$.

spikes or a constant wave form. When $\alpha>8\sqrt{3}/3$, the external crisis becomes an internal crisis. That is, both the fixed points on the bottom and middle branches of the S curve are located within the chaotic attractor. In these cases, wave forms of the two-dimensional map are predominantly fast spiking wave forms [as shown in Fig. 1(e)].

III. EFFECT OF COUPLING ON IDENTICAL BURSTERS

We now consider the effect of coupling on the solution behavior of the two-dimensional map (1), (2). Following Rulkov [14], we take the coupling through the mean field. That is, we study

$$x_{n+1,i}=\frac{\alpha_i}{1+x_{n,i}^2}+y_{n,i}+\frac{\varepsilon}{N}\sum_{j=1}^{N}x_{n,j}, \tag{6}$$

$$y_{n+1,i}=y_{n,i}-\eta(x_{n,i}-\sigma_i), \tag{7}$$

where the additional subscript i indicates the ith cell, N is the total number of cells, and ε is the strength of the coupling. In this section, we concentrate on the case $N=2$. However, the results carry over to the case $N>2$.

Figure 4 shows the solution behavior of two identical cells ($\alpha_1=\alpha_2$ and $\sigma_1=\sigma_2$), namely, those of Fig. 1(a), with $\varepsilon=0.2$. The wave form for x_2 is similar to the one shown for x_1, and bursts are synchronized (the spikes within each active phase in general are not synchronized, unless both cells start with the same initial conditions). Note that the active and silent phases are considerably longer when the cells are coupled. Of less significance, but still very noticeable, is the observation that the amplitude of the burst oscillation has increased.

These observations can easily be explained by means of a bifurcation analysis of the fast subsystem of Eqs. (6), (7). Since $y_{n,1}\approx y_{n,2}$ (not shown), we are justified in studying the fast subsystem with a *single* bifurcation parameter γ, that is,

$$x_{n+1,1}=\frac{\alpha}{1+x_{n,1}^2}+\gamma+\frac{\varepsilon}{2}(x_{n,1}+x_{n,2}), \tag{8}$$

$$x_{n+1,2}=\frac{\alpha}{1+x_{n,2}^2}+\gamma+\frac{\varepsilon}{2}(x_{n,1}+x_{n,2}), \tag{9}$$

where $\alpha=\alpha_1=\alpha_2$. The resulting bifurcation diagram for x_1 is shown in Fig. 5(a) [due to the symmetry in Eqs. (8), (9), the diagram for x_2 is identical]. Fixed points are symmetrical, that is, $x_1\equiv x_2$, and the curve of fixed points is given by $R_\varepsilon(x_n)=x_n$, where

$$R_\varepsilon(x_n)=\frac{\alpha}{1+x_n^2}+\gamma+\varepsilon x_n. \tag{10}$$

On the upper branch of steady states, pairs of period-doubling bifurcations are observed where there were single period-doubling bifurcations before. The two middle period-doubling bifurcations give rise to unstable symmetrical n-cycles and chaotic attractors, whereas the outer period-doubling bifurcations give rise to stable nonsymmetrical n-cycles and chaotic attractors. The roughly C-shaped and backward C-shaped curves emanating from the period-doubling points represent the envelopes containing the periodic or chaotic iterates of the map, based on the computation of several thousand iterates at selected values of the bifurcation parameter γ (the envelopes have been smoothed somewhat for clarity). Each of the envelopes terminates at an external crisis bifurcation. Which external crisis point most accurately predicts the return back to the silent phase for the full four-dimensional map (6), (7) depends on the initial conditions for the two cells. If the two cells are given identical initial conditions, the external crisis point associated with the symmetrical envelope most accurately predicts the return

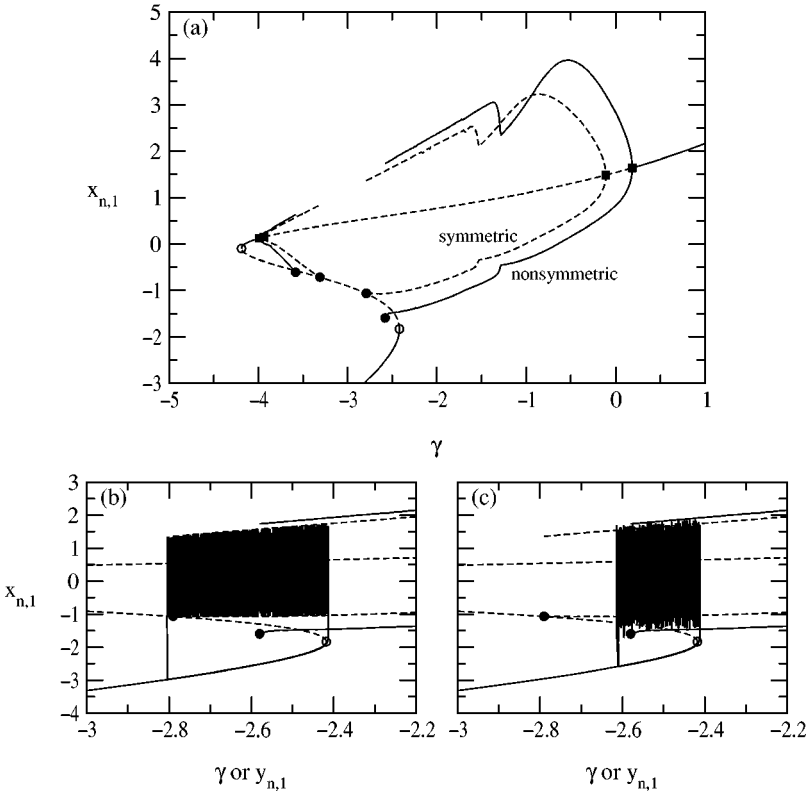

FIG. 5. (a) Bifurcation diagram for the two-cell fast subsystem (8), (9), using γ as the bifurcation parameter, with $\alpha=4.15$ and $\varepsilon=0.2$. The C-shaped and backward C-shaped curves emanating from the period-doubling points represent the envelopes containing the stable (solid) and unstable (dashed) periodic or chaotic iterates of the map after some initial transient. (b) Portion of the bifurcation diagram from (a), with a wave form of the full two-cell model (6), (7) superimposed. The two cells were given identical initial conditions. (c) As (b), but now with a wave form of two cells that were started from different initial conditions.

back to the silent phase, as shown in Fig. 5(b). However, if the two cells are given nonidentical initial conditions, the external crisis point associated with the nonsymmetrical envelope, emanating from the rightmost period-doubling point, is more accurate, as shown in Fig. 5(c).

We are now in a position to explain the effect of coupling on the length of the silent and active phases and the amplitude of the wave form observed in Fig. 4. Effectively, both characteristics are determined by the magnitude of $\gamma_{SN}-\gamma_{EC}$, where in the case of coupled cells we take γ_{EC} to be the value of γ at which the nonsymmetrical envelope terminates at an external crisis bifurcation, and γ_{SN} is as defined in the case of a single cell. When the cells are not coupled, γ_{SN} is only slightly larger than γ_{EC}, resulting in relatively short silent and active phases. Both γ_{EC} and γ_{SN} are affected by the coupling, but the net effect is that $\gamma_{SN}-\gamma_{EC}$ increases, thus lengthening both the active and silent phases, as observed. The reason for the increase in the amplitude of the wave form follows. The more γ or $y_{n,1}$ decreases during the active phase, the smaller $x_{n,1}$ upon return to the silent phase, resulting in a larger amplitude of the burst oscillation, also as observed.

The effect of the coupling strength on the locations of the pertinent bifurcation points from Fig. 5(a) is summarized in Fig. 6. As the coupling strength ε increases, both γ_{EC}, represented by the rightmost thick solid curve, and γ_{SN}, represented by the rightmost thin solid line, increase. Since γ_{SN} increases faster, the region of bistability in the bifurcation diagram is enlarged as the coupling strength increases, allowing for longer silent and active phases and, consequently, more regular bursting, as already noted in [14]. However, only Eq. (10) was studied in [14] to explain the effect of coupling and, consequently, the existence of the envelope representing stable nonsymmetrical *n*-cycles and chaotic attractors was missed. Effectively, in [14], γ_{EC} was taken to be the value of γ at which the envelope representing unstable symmetrical *n*-cycles and chaotic attractors terminates at an external crisis bifurcation. The symmetrical γ_{EC} is represented by the second-most-right thick solid curve (it joins up with the second-most-left thick solid curve as ε increases) in

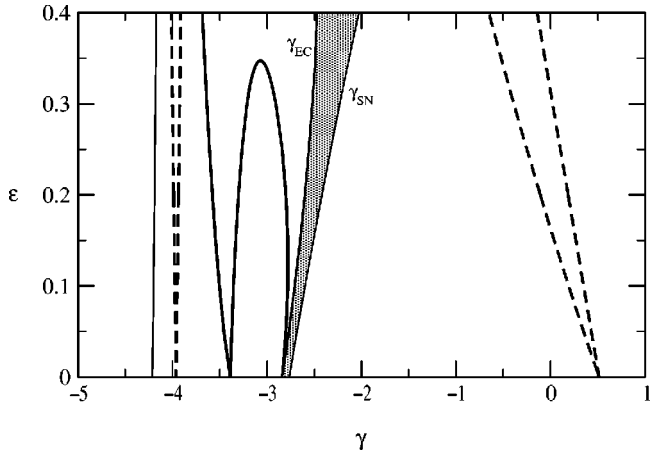

FIG. 6. Effect of the coupling strength ε on the relative locations of bifurcation points from the right half of the diagram in Fig. 5(a). Thick solid lines represent the symmetric (left) and nonsymmetric (right) external crisis bifurcations. The thin solid line represents the saddle-node bifurcation. Thick dashed lines represent the symmetric (left) and nonsymmetric (right) period-doubling bifurcations. Shading highlights the region of bistability for values of γ between γ_{EC} and γ_{SN}.

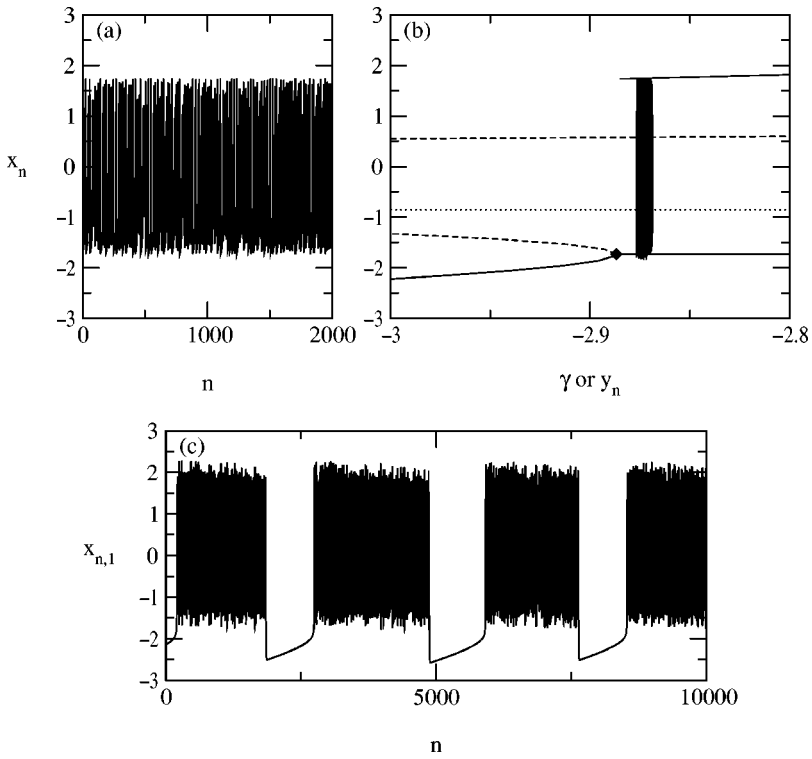

FIG. 7. Emergent bursting from coupled nonbursting cells. (a) Spiking wave form of the single-cell model (1), (2) with $\alpha=8\sqrt{3}/3$ and $\sigma=-0.85$. (b) Relevant portion of the bifurcation diagram of the corresponding single-cell fast subsystem (3), with the solution from (a) superimposed. The filled diamond indicates the simultaneous saddle-node and external crisis bifurcations. The horizonal dotted line indicates the y_n nullcline, $x_n=\sigma$. (c) Bursting wave form of the corresponding full two-cell model (6), (7) with $\varepsilon=0.2$.

Fig. 6. Thus, the role of coupling in enlarging the size of the region of bistability was exaggerated in [14]. In either case, coupling results in more regular bursting, and this is the mechanism underlying regularization, as explained in [14]. Note that in [14] a heterogenous population of cells was used. The role of heterogeneity will be examined below in Sec. V.

As alluded to above, an interesting feature of Fig. 6 is that as ε increases the two symmetrical external crisis bifurcation points approach each other. When $\varepsilon\approx0.35$, they coalesce and annihilate each other in a codimension-2 bifurcation. Thus, for $\varepsilon>0.35$, cells started off with identical initial conditions would exhibit tapered bursting, whereas the same cells started off with nonidentical initial conditions would exhibit square-wave bursting.

Of interest for the phenomenon of emergent bursting, examined below, is that the enlargement of the region of bistability occurs for a large range of coupling strengths ε. This is in contrast to the effect of (gap-junctional) coupling on previously studied continuous systems [2,11–13]. We will elaborate on this issue in the discussion in Sec. VI.

IV. BURSTING AS AN EMERGENT PHENOMENON

From the previous section, it is clear that the effect of coupling is to enlarge the region of bistability relevant for bursting behavior. In this section, we push this idea further: coupling also can *introduce* bistability to cells that do not exhibit any bistability on their own. Thus, coupling can turn spiking cells into bursting cells.

To remove the bistability in the single-cell fast subsystem, we set $\alpha=8\sqrt{3}/3$ so that $\gamma_{EC}=\gamma_{SN}$. That is, the envelope representing the minimum periodic or chaotic iterate in the bifurcation diagram of the single-cell fast subsystem, $x_n=R(R(0))$, intersects the curve of fixed points at the saddle node on the right, as shown in Fig. 7(b) (also see Fig. 3; this value of α represents the transition from external to internal crisis bifurcations and vice versa).

For this value of α, burstlike wave forms of the full single-cell model can be observed for certain choices of the slow subsystem; however, the bursting occurs on a fast time scale, and is very irregular due to the chaotic nature of the attractor for values of γ just larger than γ_{SN}. We will avoid such chaotic burstlike wave forms by changing the value of σ slightly, from $\sigma=-1$ to $\sigma=-0.85$, to obtain a spiking wave form, as shown in Fig. 7(a). The wave form is superimposed onto the bifurcation diagram of the single-cell fast subsystem in Fig. 7(b). Note that the iterates remain in the vicinity of $\gamma=y_n\approx-2.87$. This value depends on the position of the slow nullcline $x_n=\sigma$: the further the nullcline is moved upward, the further to the right the wave form will lie. The reason for this is as follows. Recall that when an iterate (x_n,y_n) of the full single-cell model falls below this nullcline, $y_{n+1}>y_n$; when it falls above the nullcline, $y_{n+1}<y_n$. The long-term behavior of the full single-cell model depends on the location of the average iterate relative to the nullcline. For values of γ near γ_{SN}, the average iterate lies below the nullcline, that is, on average, iterates will move to the right in Fig. 7(b). For values of $\gamma\gg\gamma_{SN}$, the average iterate lies above the nullcline, that is, on average, iterates will move to the left. A balance is struck somewhere in the middle.

We now couple two such spiking cells, with $\varepsilon=0.2$. The resulting bursting wave form is shown in Fig. 7(c). The reason for this new collective behavior is precisely the same one that explains the lengthening of the silent and active phases

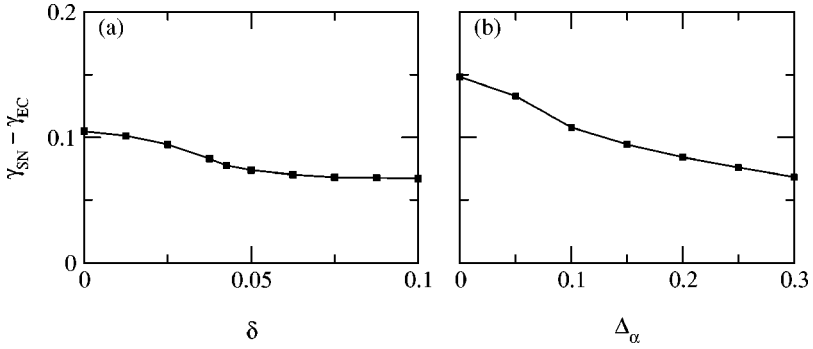

FIG. 8. Effect of heterogeneity on the size of the region of bistability in the bifurcation diagram of the fast subsystem (15), (16), measured by $\gamma_{SN}-\gamma_{EC}$. (a) Effect of heterogeneity in the slow subsystem. Parameter values are $\alpha_1=\alpha_2=8\sqrt{3}/3$ and $\varepsilon=0.2$. (b) Effect of heterogeneity in the fast subsystem. Parameter values are $\alpha_1=\hat{\alpha}+\Delta_\alpha$, $\alpha_2=\hat{\alpha}-\Delta_\alpha$, $\hat{\alpha}=4.3$, and $\varepsilon=0.2$. Filled squares indicate the values of δ and Δ_α sampled.

discussed in the previous section. Upon coupling, both the saddle-node and external crisis bifurcations move to the right, but the saddle-node bifurcation is affected more than the external crisis bifurcation so that $\gamma_{EC}<\gamma_{SN}$, and thus a region of bistability is introduced. The phenomenon of emergent bursting is very robust to a change in the coupling strength. The stronger the coupling, the larger the region of bistability, similar to the enlargement of the region of bistability shown in Fig. 6.

The single-cell fast subsystem lacks bistability only when $\alpha=8\sqrt{3}/3$. So it is natural to ask whether the emergence of more or less regular bursting persists for values of $\alpha>8\sqrt{3}/3$. Indeed, it does. For these values of α, the relevant branch of periodics/chaotics for the single-cell fast subsystem terminates at an internal crisis bifurcation, and wave forms for the full system are predominantly fast spiking [see Fig. 1(e)]. When coupled weakly, the relevant branch of periodics/chaotics, namely, the stable nonsymmetric branch, also terminates at an internal crisis bifurcation. However, as coupling increases, the internal crisis bifurcation moves toward the saddle node and then becomes an external crisis bifurcation, at which point emergent bursting can be seen. The larger α, the larger the perturbation needs to be to obtain the emergent phenomenon.

V. ROLE OF HETEROGENEITY

The emergence of bursting from nonbursting cells in previously studied continuous systems depends critically on heterogeneity in the model parameters [13]. This is the motivation to investigate the role of heterogeneity in the model parameters of the discrete map in promoting emergent bursting and, by extension, regularization [14]. We distinguish between heterogeneity in the slow and fast subsystems, but first discuss the general effect of heterogeneity and the modifications required in the computation of a bifurcation diagram.

It can be readily verified by numerical simulation that y_1 and y_2 are no longer approximately equal when $\alpha_1\neq\alpha_2$ and/or $\sigma_1\neq\sigma_2$. Thus, it no longer suffices to use γ as the *single* bifurcation parameter in the corresponding fast subsystem, as was done in Eqs. (8), (9). Two bifurcation parameters are now required to fully characterize the fast subsystem. However, y_2-y_1 is approximately constant. Thus, if we let

$$\delta=(y_1-y_2)/2, \tag{11}$$

$$y=(y_1+y_2)/2, \tag{12}$$

so that

$$y_1=y+\delta, \tag{13}$$

$$y_2=y-\delta, \tag{14}$$

then we can let $y=\gamma$ be the primary bifurcation parameter, as before, and δ be the secondary bifurcation parameter [20]. The resulting fast subsystem is

$$x_{n+1,1}=\frac{\alpha_1}{1+x_{n,1}^2}+\gamma+\overline{\delta}+\frac{\varepsilon}{2}(x_{n,1}+x_{n,2}), \tag{15}$$

$$x_{n+1,2}=\frac{\alpha_2}{1+x_{n,2}^2}+\gamma-\overline{\delta}+\frac{\varepsilon}{2}(x_{n,1}+x_{n,2}), \tag{16}$$

where $\overline{\delta}$ is the average value of δ, based on many iterations of the full two-cell system.

Although we will not do so here, the procedure to confirm the accuracy of the fast subsystem bifurcation diagram in predicting the full two-cell system behavior would be as follows. First, the full two-cell system is simulated so that $\overline{\delta}$ can be calculated *a priori*. This value of $\overline{\delta}$ is then used in Eqs. (15) and (16) to produce a bifurcation diagram with γ as the bifurcation parameter. Subsequently, an *a posteriori* check of the accuracy of the bifurcation diagram can be made by projecting the wave forms of the full system onto the bifurcation diagrams, shifted appropriately via Eqs. (13) and (14). Provided extreme heterogeneity is avoided, the bifurcation diagram thus obtained indeed can be seen to be a good predictor of the full system behavior.

Heterogeneity in the slow subsystem is achieved by letting $\sigma_1\neq\sigma_2$ in Eqs. (6) and (7). Recall that emergent burst-

ing was shown in the previous section with $\alpha_1=\alpha_2=8\sqrt{3}/3$ and $\sigma_1=\sigma_2=-0.85$. Keeping the values of $\alpha_{1,2}$ fixed, emergent bursting can be obtained for many choices of σ_1 and σ_2. The more disparate σ_1 and σ_2, the larger the resulting value of $\overline{\delta}$. Thus, in this situation, $\overline{\delta}$ can be viewed as a measure of heterogeneity in the slow subsystem. Figure 8(a) summarizes the effect of increased heterogeneity in the slow subsystem on the size of the region of bistability in the fast subsystem bifurcation diagram, measured by $\gamma_{SN}-\gamma_{EC}$. As $\overline{\delta}$ increases, the size of the region of bistability decreases (this is in accordance with the shorter bursts observed in wave forms obtained for the full two-cell system). Although heterogeneity does not significantly affect the size of the region of bistability, it is clear that heterogeneity does not promote emergent bursting, nor bursting in general, in contrast to the findings of de Vries and Sherman [13] for continuous systems.

Heterogeneity in the fast subsystem is achieved by letting $\alpha_1\neq\alpha_2$ in Eqs. (6) and (7). The effect of this type of heterogeneity can no longer be isolated in one parameter in the fast subsystem (for each choice of α_1 and α_2, a new value of $\overline{\delta}$ must be calculated). To facilitate a systematic comparison, we let

$$\alpha_1=\hat{\alpha}+\Delta_\alpha, \tag{17}$$

$$\alpha_2=\hat{\alpha}-\Delta_\alpha, \tag{18}$$

and vary Δ_α while keeping $\hat{\alpha}$ constant. Figure 8(b) summarizes the effect of increased heterogeneity (Δ_α) in the fast subsystem on the size of the region of bistability. As before, as Δ_α increases, the size of the region of bistability decreases. Thus, heterogeneity in the fast subsystem also does not promote bursting; in fact, it slightly hinders it.

VI. DISCUSSION

In this paper, we have continued the study of the simple two-dimensional map exhibiting bursting introduced by Rulkov [14]. Rulkov studied the map in the context of regularization of synchronized chaotic bursts. Although the results obtained here clarify some details of regularization, the main focus of this paper is to examine the bursting that emerges in a population of nonbursting cells when they are coupled through the mean field and to compare this phenomenon to a similar situation in continuous systems.

The analysis of Rulkov [14] revealed that the mechanism of bursting in the map is analogous to the mechanism of a certain type of bursting exhibited in many models of differential equations, namely, so-called square-wave bursting [9]. For continuous square-wave bursters, it is well known that a change in parameters can destroy the bursting behavior. Several recent papers have examined diffusively coupled networks of such nonbursting cells, and it has been shown that bursting can be recovered, albeit under certain conditions (see the Introduction for a brief review). The analogy between the mechanism underlying bursting in the map and continuous square-wave bursting provided the impetus to study emergent bursting in the map.

We began by carefully constructing a bifurcation diagram of the fast subsystem of a single bursting cell, thereby extending Rulkov's analysis of the map. Bursting in a single cell crucially depends on two model ingredients, namely, bistability between a stable fixed point and a periodic or chaotic attractor in the fast subsystem of the cell, and a slow process that can switch the system between these states.

By changing the model parameters, the bistability in the fast subsystem can be removed in a fashion similar to what has been done previously for continuous square-wave bursters [2,11–13]. When the resulting nonbursting cells were coupled through the mean field, bursting was recovered. The mechanism underlying emergent bursting was revealed by a bifurcation analysis of the coupled fast subsystem. In general, a two-parameter bifurcation analysis is required to study a coupled system. However, ideas from the study of continuous systems carried over, and it was shown that a one-parameter bifurcation analysis suffices to explain the emergent bursting phenomenon. In particular, it was found that coupling serves to perturb the system so as to reintroduce a region of bistability. The emergent bursting phenomenon is very robust: the stronger the coupling, the larger the size of the region of bistability, the longer the active and silent phases, and the more regular the bursts. This is in contrast with previously studied continuous models [2,11–13], where emergent bursting due to coupling alone is delicate, and exists only over a small range of coupling strengths. In those models, heterogeneity in the model parameters is able to rescue emergent bursting over a significant range of coupling strengths. In contrast, heterogeneity for the model studied here does not promote emergent bursting; in fact, it slightly hinders it.

Even though this paper focused on the phenomenon of emergent bursting, results were obtained that are relevant to the phenomenon of regularization of synchronized chaotic bursts [14]. In particular, the stable nonsymmetrical branch of periodics/chaotics in the bifurcation diagram of the fast subsystem of a pair of cells is shown here. Furthermore, the finding that the introduction of heterogeneity in the model parameters slightly decreases the size of the region of bistability implies that regularization is due to coupling alone.

The mechanism responsible for generating the emergent bursting shown here depends critically on the fact that the nonbursting cells were derived from bursting cells by placing them in a parameter regime not too far removed from the parameter regime where the cells exhibit bursting. As a result, the bifurcation structures of the fast subsystem for bursting and nonbursting cells are related, so that modest changes in just a few model parameters can turn a nonbursting cell into a bursting cell and vice versa. Thus, it is not surprising that a small perturbation such as that obtained from coupling between cells produces bursting from nonbursting cells. However, although the mechanism underlying emergent bursting appears similar in previously studied continuous systems and the discrete map examined here, there are some important differences. In particular, the manner in which emergent bursting does or does not persist as the coupling strength increases appears to be nongeneric, and seems

to depend on the type of equations and the type of coupling used. For example, applying diffusive coupling to the discrete bursting model does not generate emergent bursting, nor does applying mean field coupling to the continuous bursting model. In addition, whether or not heterogeneity plays a crucial role in the emergence of bursting seems to depend on the system.

Recent studies of the generation of simple oscillations in networks of electrically coupled nonoscillating cells have brought out a similar finding, namely, that heterogeneity in the model parameters may or may not be important, and that the emergent phenomenon may or may not persist as the coupling strength is increased, depending on the dynamics of the individual cells. For example, Cartwright [4] and Manor *et al.* [3] have proposed mechanisms that critically depend on heterogeneity in the cell parameters, whereas the mechanisms proposed by Sherman and Rinzel [2] and Loewenstein *et al.* [1] do not require heterogeneity. Furthermore, the emergent oscillations in [2] exist only for a restricted range of coupling, whereas they persist for arbitrarily large coupling strength in [1]. Whether the details of the various mechanisms underlying emergent oscillations and bursting can be unified by some general principles remains an open question.

The similarities and differences observed in the behavior of discrete and continuous bursting models raise some interesting questions. For example, what type of biophysical system is captured by the discrete system? Is there a direct connection between discrete and continuous bursting systems, and, if so, how can discrete maps be generated from biophysically based continuous models? The relevance of the discrete model to real biophysical systems remains to be seen. However, studying emergent bursting in a variety of systems advances our qualitative understanding of network behavior and may lead to further insight into how individual cells can function as a unit when coupled together.

ACKNOWLEDGMENT

This research was supported in part by the Natural Sciences and Engineering Research Council of Canada.

[1] Y. Loewenstein, Y. Yarom, and H. Sompolinsky, Proc. Natl. Acad. Sci. U.S.A. **98**, 8095 (2001).
[2] A. Sherman and J. Rinzel, Proc. Natl. Acad. Sci. U.S.A. **89**, 2471 (1992).
[3] Y. Manor, J. Rinzel, I. Segev, and Y. Yarom, J. Neurophysiol. **77**, 2736 (1997).
[4] J.H.E. Cartwright, Phys. Rev. E **62**, 1149 (2000).
[5] P.M. Dean and E.K. Matthews, J. Physiol. (London) **210**, 255 (1970).
[6] R.S.K. Wong and D.A. Prince, J. Neurophysiol. **45**, 86 (1981).
[7] M. Deschênes, J.P. Roy, and M. Steriade, Brain Res. **239**, 289 (1982).
[8] J. Rinzel, in *Ordinary and Partial Differential Equations*, edited by B. D. Sleeman and R. J. Jarvis, Lecture Notes in Mathematics Vol. 1151 (Springer, New York, 1985), pp. 304–316.
[9] J. Rinzel, in *Mathematical Topics in Population Biology, Morphogenesis, and Neurosciences*, edited by E. Teramoto and M. Yamaguti, Lecture Notes in Biomathematics Vol. 71 (Springer, New York, 1987), pp. 267–281.
[10] P. Smolen, J. Rinzel, and A. Sherman, Biophys. J. **64**, 1668 (1993).
[11] A. Sherman, Bull. Math. Biol. **56**, 811 (1994).
[12] G. de Vries and A. Sherman, J. Theor. Biol. **207**, 513 (2000).
[13] G. de Vries and A. Sherman, Bull. Math. Biol. **63**, 371 (2001).
[14] N.F. Rulkov, Phys. Rev. Lett. **86**, 183 (2001).
[15] J.L. Hindmarsh and R.M. Rose, Proc. R. Soc. London, Ser. B **221**, 87 (1984).
[16] M. Pernarowski, SIAM (Soc. Ind. Appl. Math.) J. Appl. Math. **54**, 814 (1994).
[17] E.M. Izhikevich, Int. J. Bifurcation Chaos Appl. Sci. Eng. **10**, 1171 (2000).
[18] R.M. May, Nature (London) **261**, 459 (1976).
[19] G. de Vries, J. Nonlinear Sci. **8**, 281 (1998).
[20] G. de Vries, A. Sherman, and H.-R. Zhu, Bull. Math. Biol. **60**, 1167 (1998).